Fig. 5. Contributions to the fields in the $x = 0$ plane for the linearly blended rolled edge reflector.
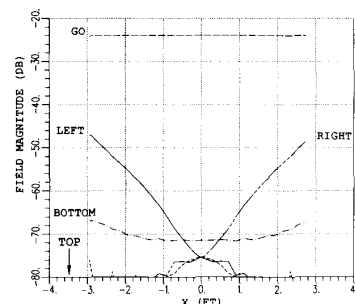

Fig. 6. Contributions to the fields in the $y = 6.5$ ft plane for the linearly blended rolled edge reflector.

Another advantage of the NUTD is computational efficiency. Since the NUTD requires PO line integrations, the total CPU time required to carry out the integration is directly proportional to frequency. POSI, on the other hand, requires surface integration; thus, the CPU time is proportional to the frequency squared. For the software used to generate the results appearing here, running on a VAX 8550 computer, it was found that POSI (using one-tenth-wavelength patches) required about 150 CPU-s per field point, while the NUTD required about 3 CPU-s. In fact, practical considerations often make it necessary to perform the POSI calculations on a supercomputer, even at the lowest frequencies of interest. The NUTD method offers considerable improvement in this respect.

IV. CONCLUSION

In this communication, an efficient technique for analyzing the performance of compact range reflectors with blended rolled edges was presented. The technique is based on the UTD concept, where the diffraction coefficients are obtained numerically using a corrected PO line integration method. It was shown that this approach yields results which are in good agreement with the corrected POSI method for the fields in the target zone. Furthermore, the numerical UTD is much more efficient than the POSI method. The numerical UTD method also provides diagnostic information on the effects of individual scattering mechanisms.

APPENDIX

For completeness, the various parameters of the reflectors considered here are given in the following. For a more detailed explanation of these parameters, the reader is referred to [6]. For both the linearly and cosine-blended rolled edge reflectors, the junction contour dimensions are $r_e = 3.0$ ft, $x_{left} = -3.0$ ft, $x_{right} = 3.0$ ft, $y_{bottom} = 3.5$ ft, and $y_{top} = 9.5$ ft. The feed tilt angle for both reflectors is $\alpha = 24.45°$. The parameters for the linearly blended rolled edge are $a_e = 0.500$ ft, $b_e = 1.395$ ft, $x_m = 11.151$ ft, and $\gamma_m = 120°$. For the cosine-blended rolled edge, $a_e = 0.500$ ft, $b_e = 2.204$ ft, $x_m = 10.983$ ft, and $\gamma_m = 120°$. The rolled edge parameters were assumed to be the same for all points along the junction contour.

REFERENCES

[1] R. G. Kouyoumjian and P. H. Pathak, "A uniform geometrical theory of diffraction for an edge in a perfectly conducting surface," Proc. IEEE, vol. 62, pp. 1448-1461, Nov. 1974.

[2] C. W. I. Pistorius, "New main reflector, subreflector and dual chamber concepts for compact range applications," Ph.D. dissertation, Ohio State Univ., Columbus, OH, 1986.

[3] P. H. Pathak, "The dyadic diffraction coefficient for a perfectly conducting wedge," Masters thesis, Ohio State Univ., Columbus, OH, 1970.

[4] S. W. Ellingson, I. J. Gupta, and W. D. Burnside, "Analysis of blended rolled edge reflectors using numerical UTD," Ohio State Univ. ElectroSci. Lab., Columbus, OH, Tech. Rep. 721929-2, June 1989.

[5] I. J. Gupta and W. D. Burnside, "A physical optics correction for backscattering from curved surfaces," IEEE Trans. Antennas Propagat., vol. AP-35, pp. 553-561, May 1987.

[6] I. J. Gupta, K. P. Ericksen, and W. D. Burnside, "A method to design blended rolled edges for compact range reflectors," IEEE Trans. Antennas Propagat., vol. 38, pp. 853-861, June 1990.

[7] I. J. Gupta, C. W. I. Pistorius, and W. D. Burnside, "An efficient method to compute spurious endpoint contributions in PO solutions," IEEE Trans. Antennas Propagat., vol. AP-35, pp. 1426-1435, Dec. 1987.

Mutual Coupling Compensation in Small Array Antennas

HANS STEYSKAL, MEMBER, IEEE, AND
JEFFREY S. HERD, MEMBER, IEEE

Abstract—A technique to compensate for mutual coupling in a small array is developed and experimentally verified. Mathematically, the compensation consists of a matrix multiplication performed on the received signal vector. This, in effect, restores the signals as received by the isolated elements in the absence of mutual coupling. The technique is most practical for digital beamforming antennas where the matrix operation can be readily implemented.

INTRODUCTION

The radiation pattern of an array of identical antenna elements is usually taken to be the product of an element factor and an array factor, based on the presumption that all elements have equal radiation patterns. Unfortunately, this may not be true for a practical array, where, due to mutual coupling, each element "sees" a different environment. The nature of the error thus incurred can be displayed by expressing the individual array element pattern $f_n(u)$

as the sum of one average array element pattern $f^a(u)$ and a pattern deviation $\delta f_n(u)$, which leads to the total array pattern

$$F(u) = \sum_n a_n f_n(u) e^{jnkdu}$$

$$= f^a(u) \sum_n a_n e^{jnkdu} + \sum_n a_n \delta f_n(u) e^{jnkdu}. \quad (1)$$

Here $a_n = |a_n| \exp(j\phi_n)$ denotes the complex element weight, k the wavenumber, d the uniform element spacing and u the sine of the angle θ from broadside, respectively. The first term on the right side of (1) represents the idealized pattern, and the second represents the error.

One effect of this error pattern is to introduce a noise floor that precludes synthesis of high-quality patterns with very low sidelobes or deterministic pattern nulls. Other effects appear in signal processing arrays, such as adaptive or superresolution systems, which can be extremely sensitive to small errors due to the nonlinear processing involved. Since real-life signal processing arrays usually are comparatively small arrays, where element pattern differences are relatively large, this is a significant problem.

It is clear from (1) that the element coefficients $\{a_n\}$ always can be chosen such as to compensate for the pattern error at one particular angle. It is less obvious that the error normally can be corrected for all angles simultaneously. Furthermore, since this correction is scan independent, it also applies in the case of electronic scanning. It is the purpose of this communication to discuss such a technique and to present some experimental results.

The key to the technique is an alternative formulation to (1), which recognizes that 1) any composite array pattern can be considered as a weighted sum of the isolated element patterns and 2) the effect of mutual coupling is simply to parasitically excite all elements, even though only one element is driven. Thus, by driving the array with modified element excitations, such that the desired array aperture distribution is obtained in the presence of these parasitics, the mutual coupling can be compensated for. This compensation principle has been reported for a slot array [1] and dipole arrays [2]-[4]. The former is the only one that considers the case of scanning and presents some experimental data; all four rely on computed coupling coefficients. The present study differs in that it rephrases the approach for the receiver mode, appropriate for a digital beamforming antenna where the technique is most practical, and it describes an alternative method to determine the mutual coupling coefficients, that does not require analytically simple or reciprocal array elements. It also presents experimental data for a scanned waveguide array.

THEORY

We consider an array of single-mode elements, meaning that the element aperture currents (electric or magnetic) may change in amplitude but not in shape, as a function of radiation direction. In the receive mode, the signal at the output of the individual antenna element has several constituents: a dominant one due to the direct incident plane wave, and several lesser ones due to scattering of the incident wave at neighboring elements. As depicted in Fig. 1, we can write the received signal at element m as

$$v_m(u) = c_{mm} E_m f^i(u) + \sum_{n, m \neq n} c_{mn} E_n f^i(u). \quad (2)$$

The incident field E_m at element m impresses an aperture current amplitude $E_m f^i(u)$, where $f^i(u)$ is the isolated element pattern, i.e., the pattern of the current mode assumed in the element aperture. This aperture current will produce an element output voltage $c_{mm} E_m f^i(u)$, where c_{mm} denotes the coupling from the aperture to the output transmission line. The effect of the neighbor-
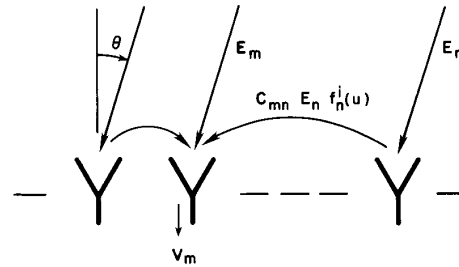

Fig. 1. The received signal v_m at element m consists of a directly transmitted and several scattered components.

ing elements is described similarly, with c_{mn} denoting the coupling of aperture mode n to element output m. From a mathematical point of view, (2) simply expresses the linear relationship between the aperture excitations and the element output voltages. The physical meaning of the c_{mn} will be discussed below.

We introduce the notation

$$E_n f^i(u) = v_n^d(u) \quad (3)$$

since this represents the desired, coupling-unperturbed signal received by the single element at the aperture. Thus for our uniformly spaced array of identical elements

$$E_0 e^{jnkdu} f^i(u) = v_n^d(u) \quad (3a)$$

where E_0 is the amplitude of the plane wave incident from direction u.

Substituting (3) in (2) leads to

$$\begin{pmatrix} v_1(u) \\ \vdots \\ v_N(u) \end{pmatrix} = (c_{mn}) \begin{pmatrix} v_1^d(u) \\ \vdots \\ v_N^d(u) \end{pmatrix}. \quad (4)$$

On the left side, the vector $\mathbf{v}$ represents the coupling perturbed signals $\{v_n\}$ at the element output ports, which via the coupling matrix $\mathbf{C}$ is related to the vector $\mathbf{v}^d$, representing the unperturbed desired signals $\{v_n^d\}$. Thus compensation for the mutual coupling can be accomplished by simply multiplying the received signal $\mathbf{v}$ by the inverse coupling matrix $\mathbf{C}^{-1}$,

$$\mathbf{v}^d = \mathbf{C}^{-1} \mathbf{v}. \quad (5)$$

This concept is depicted in Fig. 2, where a network corresponding to $\mathbf{C}^{-1}$ is attached to the array antenna. Note that the coupling compensation is scan independent, i.e., the same matrix $\mathbf{C}^{-1}$ applies universally for all directions of the incoming wave, as a consequence of our single-mode assumption. Multimode elements, as considered in [2]-[4], would require a scan dependent coupling compensation.

When the received and compensated signals $\mathbf{v}^d$ are weighted and summed in the conventional beamforming network, shown in Fig. 2, we obtain the array pattern $F(u)$, defined as the ratio of the output voltage and the incident wave amplitude E_0,

$$F(u) = \frac{1}{E_0} \sum_n a_n v_n^d = f^i(u) \sum_n a_n e^{jnkdu}. \quad (6)$$

The array pattern (6) now has the desired form of a product of an element factor and an array factor. A comparison with (1) shows that, with the transformation performed, we have succeeded in dissolving the error pattern, the second term on the right side of (1).

The matrix $\mathbf{C}^{-1}$ may be difficult or impractical to realize by an analog network, but it can be readily realized in a digital beamform-
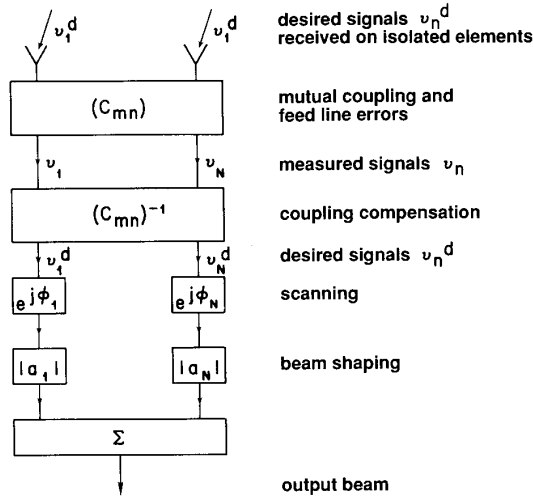
Fig. 2. Illustration of coupling compensations and beamforming in an array antenna. Interelement coupling at the array face, represented by (c_{mn}), leads to received signals v_n at array element outputs, that are linear combinations of the desired, coupling-unperturbed signals v_n^d. Multiplication by $(c_{mn})^{-1}$ restores these signals, which are then weighted and summed to form the desired beam.

ing antenna system. It then allows all subsequent beamforming operations to be performed with ideal element signals, such as are usually assumed in pattern synthesis.

DETERMINATION OF THE MUTUAL COUPLING COEFFICIENTS

There appear to be two different methods to determine the coupling coefficients—one by Fourier decomposition of the measured array element patterns and another by coupling measurements between the array ports. The former requires driving the antenna only in one mode, either transmit or receive, and thus applies to nonreciprocal antenna systems. The latter requires driving each element in both modes and therefore is less practical, as discussed below.

In the Fourier decomposition method we measure the complex voltage patterns $g_m(u)$ of the elements in their array environment, cf. (2).

$$g_m(u) = \frac{v_m(u)}{E_0} = f^i(u) \sum_n c_{mn} e^{jnkdu} \qquad (7)$$

and, recognizing that the c_{mn} are the Fourier coefficients of these patterns, determine these coefficients numerically according to

$$c_{mn} = \frac{1}{2\pi} \int_{-\pi/kd}^{\pi/kd} \frac{g_m(u)}{f^i(u)} e^{-jnkdu} \, du. \qquad (8)$$

In order to do this, $f^i(u)$ must not have a null in the integration interval. However, since the isolated element pattern normally is very wide, this is no serious limitation. Another restriction on (8) is that the element spacing be larger than $\lambda/2$. Otherwise the integration interval extends beyond visible space, i.e., beyond the interval $-1 < u < 1$ where $g_m(u)$ and $f^i(u)$ are known.

For the case of element spacings $d < \lambda/2$ we can still perform a spectral analysis of

$$\frac{g_m(u)}{f^i(u)} = \sum_n c_{mn} e^{jnkdu} \qquad (9)$$

to determine the coefficients c_{mn}, but the convenient orthogonality
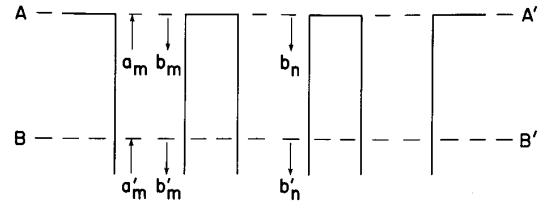

Fig. 3. Illustration of the scattering matrices **S** and **S**' of the array. Line sections between aperture plane AA' and terminal plane BB' are matched and reciprocal, with transmission coefficients t_n.

of the harmonic functions is lost and accuracy becomes a major issue.

An advantage of this method is that it does not require reciprocal antenna elements. Thus, it is applicable to receive-only arrays, such as used for digital beamforming, where the element includes an entire microwave receiver. Furthermore, any channel imbalances, i.e., differences in insertion amplitude and phase between the element aperture and the element output terminal, manifest themselves in the self-terms c_{mm} and are also compensated for. In this sense the technique is similar to a conventional array calibration.

In the second method, the matrix **C** is obtained from the related scattering matrix $\mathbf{S} = (s_{mn})$ of the array. This relation is developed here for the simplest case of a waveguide array fed by matched generators. For the general case the relation is complicated and not very useful.

We consider a uniformly spaced array of waveguide elements, shown in Fig. 3, and determine the array element pattern of element m. This element is excited with a wave of amplitude a_m, all other elements are passive. Assuming a reference plane AA' for the antenna element terminals that coincides with the element apertures, the aperture voltages thus are

$$v_n = \left(\delta_{nm} + s_{nm} \right) a_m \qquad (10)$$

where the Kronecker delta $\delta_{mn} = 1$ for $n = m$, and $= 0$ otherwise.

The radiated far field

$$E_m = \sum_n v_n f^i(u) \frac{e^{-jkr_n}}{r_n}$$

$$\simeq a_m f^i(u) \frac{e^{-jkr_0}}{r_0} \sum_n \left(\delta_{nm} + s_{nm} \right) e^{jnkdu} \qquad (11)$$

where r_n is the distance of element n to the observation point and the usual far-field approximations have been made. Comparing this expression with (7) and requiring that the transmit and receive patterns are identical, shows that

$$c_{mn} = \delta_{nm} + s_{nm}$$

apart from a constant factor of no interest. Thus

$$\mathbf{C} = \mathbf{I} + \mathbf{S} \qquad (12)$$

where **I** denotes the identity matrix.

In real arrays, the scattering matrix cannot normally be measured directly at the element apertures, as assumed above, but only from a reference plane a certain distance behind the apertures. A more realistic case therefore is as shown in Fig. 3, where sections of transmission line are included between the apertures and the reference plane BB', from which the modified scattering matrix **S**' is measured. These feed lines have different insertion phase and loss. However, for simplicity, we still assume them to be matched and

reciprocal, so that they can be characterized by single transmission coefficients t_m.

Defining a diagonal matrix T,

$$T = (t_m \delta_{mn}) \tag{13}$$

it is easy to show that

$$S' = TST \tag{14}$$

and, from (4) and (12), that the received signals at plane BB' are

$$v' = T(I + S)v^d = (T + S'T^{-1})v^d. \tag{15}$$

The modified coupling matrix C' at plane BB' thus is

$$C' = T + S'T^{-1} \tag{16}$$

which shows that in this case we need to measure not only the scattering matrix S' but also the transmission coefficients $\{t_m\}$. This may or may not be possible, depending on the design of the actual array.

Clearly for the general case, where the feed lines between the element apertures and output terminals are not matched, the required measurements become still more extensive. Thus, measurement of the network parameters, which intuitively would seem less complicated than pattern measurements with Fourier decompositions, in reality often is the less practical method.

EXPERIMENTS

The coupling compensation technique outlined in the preceding section was applied to an eight-element linear array of X-band rectangular waveguides in a ground plane. Each element was in turn a column of 8 rectangular waveguides in a common H-plane, combined via a fixed 1:8 power divider. The array axis thus was parallel to the E-plane and in this plane the element spacing $d = 1.25$ cm $= 0.517$ λ. The isolated element pattern corresponds to a normalized uniform aperture distribution

$$f^i(u) = \frac{\sin \dfrac{kl}{2} u}{\dfrac{kl}{2} u} \tag{17}$$

where l is the interior waveguide height, in our case $l = 1.02$ cm $= 0.417$ λ.

The complex voltage patterns $g_m(u)$ of the array elements were measured under matched load conditions, and recorded at $1/2$-degree intervals with a digital receiver. The coupling coefficients c_{mn} were then numerically evaluated according to (8) and the inverse matrix C^{-1} was computed. In a second, similar measurement, the received voltages $v_m(u)$ were again recorded. Then, in an off-line simulation of a digital beamforming system, they were multiplied with C^{-1} for coupling compensation, and amplitude and phase weighted for pattern shaping and scanning, as shown in Fig. 2.

Examples of element patterns for a central and an edge element are shown in Fig. 4. We note that there is indeed a considerable difference in shape, which is attributable to mutual coupling effects, and also in overall power level, which mainly is due to a difference in feed line losses.

In Figs. 5(a) and 5(b) we show synthesized 30-dB Chebyshev patterns as obtained without and with the mutual coupling compensation. Apparently the compensation technique gives about 10 dB improvement in sidelobe level, with the result that the actual pattern is quite close to the theoretical one. The remaining difference
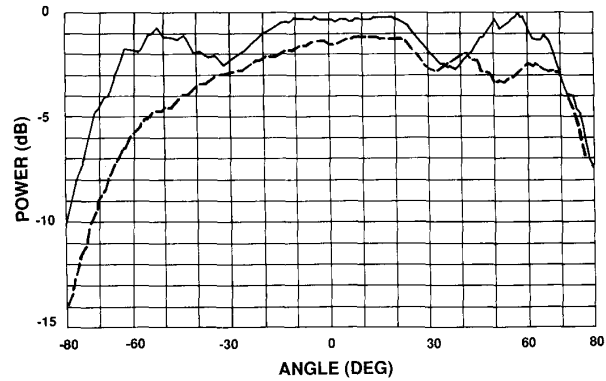

Fig. 4. Measured pattern magnitudes $|g_m(\theta)|$ for center (—) and edge (--) elements of the eight-element array.
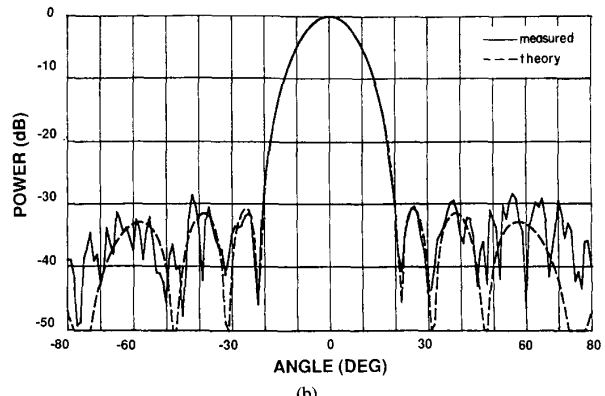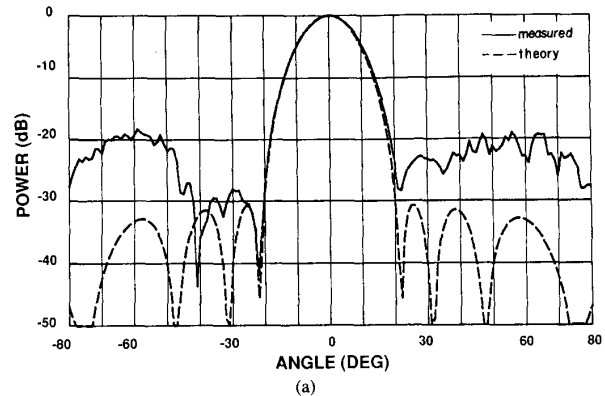

(a)

(b)

Fig. 5. 30-dB Chebyshev pattern without and with coupling compensation. Scan angle 0°.

indicates that the array excitation tolerance errors equal about -35 dB in amplitude and 1° in phase.

Figs. 6(a) and 6(b) show the same 30-dB Chebyshev patterns scanned to $-30°$. Without compensation the sidelobe level is still limited to about -20 dB. When we apply the compensation, the same C^{-1} matrix multiply as for the broadside pattern, we again reduce the sidelobe level by about 10 dB and closely reproduce the desired pattern.
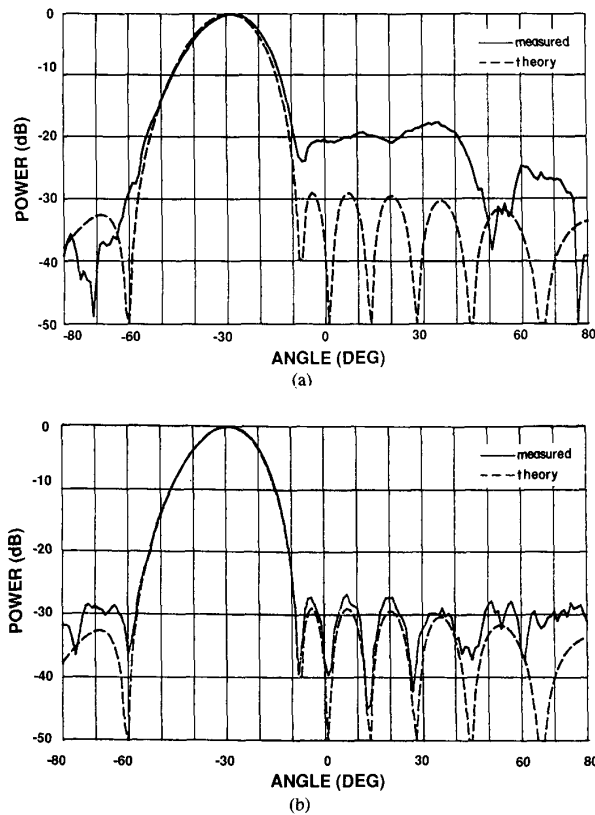
ANGLE (DEG)

(a)

ANGLE (DEG)

(b)

Fig. 6. 30-dB Chebyshev pattern without and with coupling compensation. Scan angle $-30°$.

Conclusion

We have developed and experimentally verified a technique to compensate for mutual coupling in an array. The technique should be helpful primarily for small arrays, where the array element patterns differ significantly due to edge effects. In large arrays, where each element sees essentially the same environment, these effects become negligible.

Mathematically, the compensation consists of a matrix multiplication performed on the received signal vector. This, in effect, restores the signals as received by the isolated elements in the absence of coupling. An attractive feature is that this matrix is fixed and thus is valid for all desired pattern shapes and scan directions. Although it may be difficult to realize in analog form, it can be readily implemented in a digital beamforming antenna system.

References

[1] T. Chiba, "On the realization of the synthesized pattern of scanning arrays," presented at Int. Conf. on Radar, Paris, France, Dec. 1978.
[2] B. Strait and K. Hirasawa, "Array design for a specified pattern by matrix methods," *IEEE Trans. Antennas Propagat.*, vol. AP-17, Mar. 1969.
[3] N. Inagaki and K. Nagai, "Exact design of an array of dipole antennas giving the prescribed radiation patterns," *IEEE Trans. Antennas Propagat.*, vol. AP-18, Jan. 1971.
[4] Y-W. Kang and D. Pozar, "Correction of error in reduced sidelobe

synthesis due to mutual coupling," *IEEE Trans. Antennas Propagat.*, vol. AP-33, Sept. 1985.

An Expression for the Mutual Impedance of Coplanar, Orthogonal Surface Patches

GRANT DAVIS

Abstract—An exact formula is given for the impedance of two orthogonal, coplanar, piecewise sinusoidal surface patches. This algorithm is then implemented with a previously published expression for parallel, coplanar, piecewise sinusoidal surface patches. The two algorithms are then used to generate the complete impedance matrix for a rectangular plate.

I. Introduction

The piecewise sinusoidal basis function has been used extensively since its development by Richmond [1] in 1974. Richmond derived an exact solution for the impedance between two infinitely thin filamentary monopoles. This solution is both relatively simple and compact. Impedance elements derived from other basis functions normally require a time-consuming double integral. Newman and Pozar [2] exploited this efficient algorithm to produce the versatile electromagnetic surface patch (ESP) code. ESP uses the electric field integral equations to compute currents for conducting surfaces. Their program, instead of calculating the often very slowly converging four-dimensional integral associated with the impedances between surface patches, needed only to calculate a much easier two-dimensional integral. This was accomplished by modeling a surface patch with a set of infinitely thin piecewise sinusoidal filaments and then using Richmond's wire code.

Numerical difficulty still exists in evaluating these final two integrals when the test and basis patches are very near one another. The impedance between two filaments as they approach one another is logarithmically singular or worse. A considerable amount of thought has derived the solution of an "equivalent radius" for obtaining an accurate impedance between two filaments [3]. Upon Singh and Adams' analysis [4], Newman and Pozar [5], [6] extended the "equivalent radius" concept with their "equivalent separation." This technique does improve the self-impedance term but is by no means perfect.

The lack of precision of this technique has been demonstrated by the calculation of the "exact" solution, which Janaswamy [7] has published for parallel rectangular coplanar surface monopoles. An algorithm is presented in this communication which extends the set of "exact" solutions to the impedance between a rectangular surface dipole patch and a rectangular, coplanar, orthogonal surface monopole patch with assumed piecewise sinusoidal current distribution. This solution expresses the surface–surface impedance as the sum of one-dimensional nonsingular integrals and exponential integrals. Janaswamy observed large relative errors when the parallel surface patches were nearly touching. Similar errors have been